



Geophysical Research Letters

RESEARCH LETTER

10.1002/2014GL059423

Key Points:

- Knobs detected with patchy phyllosilicates may be eroded remnants of highlands
- Hydrated silica in the younger plains formed in localized aqueous environments
- The hydrated minerals indicate less intensive aqueous alteration through time

Correspondence to:

L. Pan,
lpan@caltech.edu

Citation:

Pan, L., and B. L. Ehlmann (2014), Phyllosilicate and hydrated silica detections in the knobby terrains of Acidalia Planitia, northern plains, Mars, *Geophys. Res. Lett.*, 41, 1890–1898, doi:10.1002/2014GL059423.

Received 26 JAN 2014

Accepted 28 FEB 2014

Accepted article online 4 MAR 2014

Published online 26 MAR 2014

Phyllosilicate and hydrated silica detections in the knobby terrains of Acidalia Planitia, northern plains, Mars

L. Pan¹ and B. L. Ehlmann^{1,2}

¹Division of Geological and Planetary Science, California Institute of Technology, Pasadena, California, USA, ²Jet Propulsion Laboratory, California Institute of Technology, Pasadena, California, USA

Abstract Here we report detections of Fe/Mg phyllosilicates and hydrated silica in discrete stratigraphic units within the knobby terrains of Acidalia Planitia made using data acquired by Compact Reconnaissance Imaging Spectrometer for Mars. Fe/Mg phyllosilicates are detected in knobs that were eroded during southward retreat of the dichotomy boundary. A second later unit, now eroded to steep-sided platforms embaying the knobs, contains hydrated silica, which may have formed via localized vapor weathering, thin-film leaching, or transient water that resulted in surface alteration. These are then overlain by smooth plains with small cones, hypothesized to be mud volcanoes which previous studies have shown to have no hydrated minerals. In spite of Acidalia's location within the putative northern ocean, collectively, the data record a history of aqueous processes much like that in the southern highlands with progressively less intensive aqueous chemical alteration from the Noachian to Amazonian.

1. Introduction

In contrast to the southern highlands, the northern plains have been topographically low throughout most of the history of Mars and have served as a depositional center that preserves a geologic record from the Noachian to present. The dichotomy between the southern highlands and northern plains formed in the pre-Noachian [Frey *et al.*, 2002], and the heavily cratered Noachian basement was subsequently overlain by Hesperian and Amazonian lavas [Head *et al.*, 2002] and sediments [Tanaka, 1997]. Presently, the northern plains are largely covered by the Vastitas Borealis Formation generally thought to be sediments derived from highland rocks [Tanaka *et al.*, 2003; Kreslavsky and Head, 2002]. An outstanding question is the prevalence of water in the lowlands, i.e., whether they hosted an ancient ocean for long periods of Mars history [Parker *et al.*, 1993; Head *et al.*, 1999] or were only intermittently flooded by discharge from outflow channels [Tanaka *et al.*, 2001; Carr and Head, 2003]. Inspection of hydrated minerals in the northern plains may help resolve the nature of aqueous processes experienced and improve our understanding of the timing and prevalence of liquid water throughout Mars history.

Previous missions have characterized northern plains composition. Data from the Thermal Emission Spectrometer onboard Mars Global Surveyor showed a relatively silica-rich surface compared to basalts found in the southern highlands [Bandfield *et al.*, 2000; Christensen *et al.*, 2001], which was first proposed to originate from andesitic volcanism [Bandfield *et al.*, 2000] but later suggested to result from aqueous alteration of basalt, ranging from intensive alteration to form phyllosilicates [Wyatt and McSween, 2002] to high-silica coatings on basalt [Kraft *et al.*, 2003; Michalski *et al.*, 2005] or basaltic glass [Horgan and Bell, 2012]. In contrast to the southern highlands, later visible/shortwave infrared OMEGA data showed no evidence for widespread hydrated silicates in the north. Instead, the plains were characterized by a spectral signature typical of coated materials, which is downward sloping to longer wavelengths [Mustard *et al.*, 2005]. Higher spatial resolution data from the Compact Reconnaissance Imaging Spectrometer for Mars (CRISM) onboard Mars Reconnaissance Orbiter enabled recent discoveries of mafic minerals (olivine and pyroxene) associated with crater walls and ejecta [Salvatore *et al.*, 2010] and hydrated silicate detections in large craters [Carter *et al.*, 2010]. These observations collectively suggested a stratigraphy of altered Noachian basement, covered by unaltered Hesperian lavas, covered by later mantling materials; however, the association of all these materials with craters led to some ambiguity in formation history, e.g., with regard to the timing of aqueous alteration. Here we examine the composition and morphology of in-place stratigraphy in the Acidalia Planitia region to better understand the history of geologic processes and aqueous alteration in Mars' northern plains.

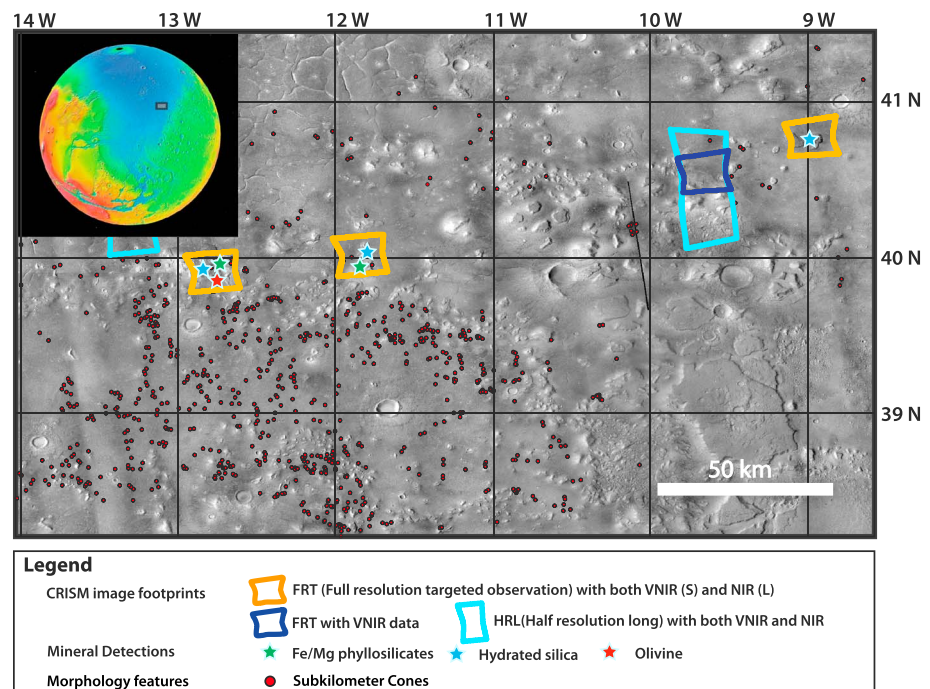


Figure 1. Geological context of the knobby terrains in Acidalia. Background image is a 38-image mosaic with data from Context Camera (CTX); colored boxes show the CRISM image footprints with stars representing hydrated mineral detections. Red dots show the geographical distribution of cones. The knobby features are larger and are located both within and to the north of the cones.

2. Geologic Context and Study Area

Acidalia Planitia terrains include small conical features and mound-shaped knobs with intriguing origins. The knobs and cones (Figure 1) of Acidalia/Chryse Planitia were first recognized in Viking imagery [Frey *et al.*, 1979] and show diverse sizes and morphology. Here we refer to “knobs” as mound-like features that are 1–5 km across, while “cones” are subkilometer features usually with a summit pit (annotated in Figure 1). At least five hypotheses have been proposed for the origin of the cones found within Amazonian terrains, including cinder cones of volcanic origin [Frey and Jarosewich, 1982], rootless cones (or pseudocraters) formed by lava flows interacting with groundwater [Frey *et al.*, 1979; Frey and Jarosewich, 1981], pingos which are ice-cored mounds formed due to freeze-thaw changes [Lucchitta, 1981], mud volcanoes formed by pressurized release of a liquid slurry of fine-grained materials [Farrand *et al.*, 2005; Oehler and Allen, 2010], or geysers and springs [Farrand *et al.*, 2005]. Possibly more than one process is involved in the formation of these features [McGill, 2005]. Larger mounds were previously suggested to be eroded remnants from the southern highlands [Tanaka, 1997; Nimmo and Tanaka, 2005; McGill, 2005], but recent studies using High-Resolution Imaging Science Experiment (HiRISE) images gave rise to the hypothesis that they form as tuyas in close relationship to chains of small cones within the plains, during volcano-ice interaction [Martinez-Alonso *et al.*, 2011].

Previous works that looked at conical features using CRISM data showed ferrous and ferric variations and hints of olivine and augite features but did not find hydrated minerals [Oehler and Allen, 2010; Farrand *et al.*, 2011]. Here we report hydrated mineral detections, including Fe/Mg phyllosilicates and hydrated silica that are related to the knobby terrains near the eastern margin of the Acidalia Planitia. We also discuss the formation mechanisms for these hydrated minerals and their implications for the geological processes the northern plains have undergone.

3. Methods

Mineral detections are made using near-infrared spectra of wavelengths 1 μm to 2.6 μm from data (Figure 1) acquired by the CRISM imaging spectrometer. Image cubes, converted to CRISM I/F [Murchie *et al.*, 2009],

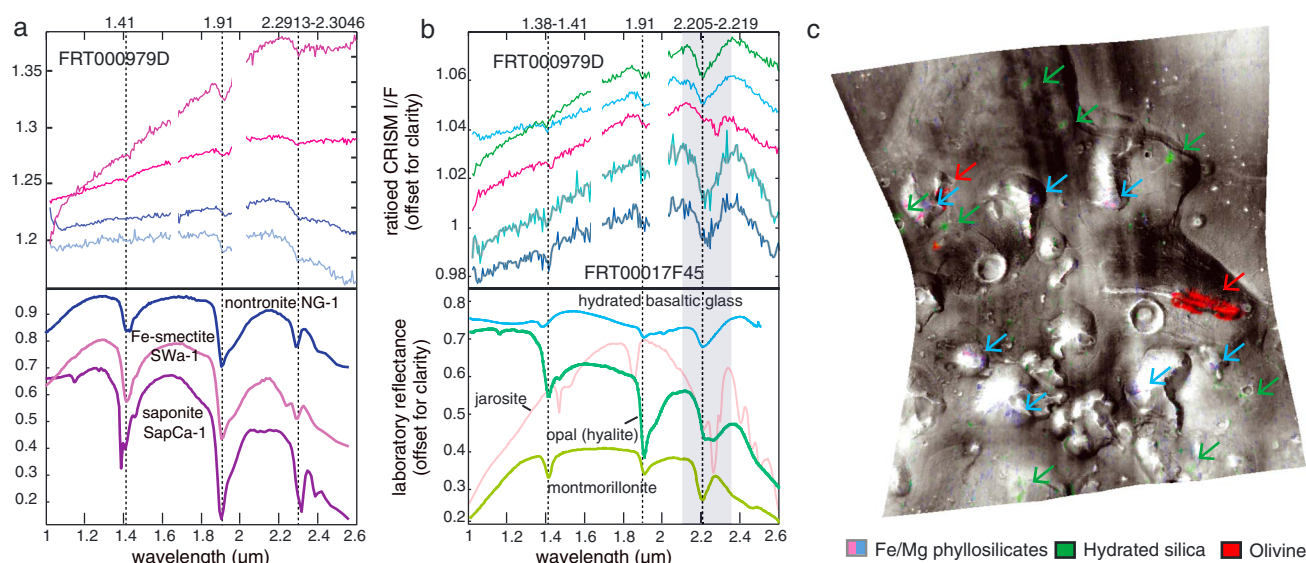


Figure 2. Representative spectra of the hydrated mineral detections in Acidalia knobby terrains. (a) top: Representative Fe/Mg phyllosilicate spectra in the scene. bottom: Fe and Mg smectite laboratory spectra. (b) top: Two hydrated silica for each image. Pink one is the doublet material. bottom: Laboratory spectra of minerals with 2.2 μm absorption band. Light gray band shows the width of the 2.2 μm band in the detections. (c) CRISM image FRT0000979D with colored parameter [R: OLINDEX2, G: BD2200, B: D2300] showing composition overlain on a gray scale background. Note the different occurrences of the Fe/Mg phyllosilicates and the hydrated silica and the linear, high-standing morphology of largest olivine exposure.

were processed using atmospheric correction and noise removal procedures described in *Ehlmann et al.* [2009]. Spectra derived from pixels in processed CRISM images were averaged over a small area and ratioed to the average spectra of a spectrally “bland” region to highlight the different mineral phases within the target region. High-resolution images taken by the Context Camera (CTX) [Malin et al., 2007], the High-Resolution Imaging Science Experiment (HiRISE) [McEwen et al., 2007], and digital elevation models derived from these using NASA Ames Stereo Pipeline [Moratto et al., 2010] were coregistered and overlain with CRISM detections to better understand the geological settings.

4. Minerals Identified

Using the ratioed spectra, mafic minerals and hydrated silicates were identified by electronic transition absorptions caused by Fe in octahedral sites and vibrational absorptions caused by overtones and combinations related to H₂O and OH in the mineral structure. Three distinct spectral classes were initially identified using parameter maps [Pelkey et al., 2007] in the region near Acidalia/Chryse dichotomy: olivine with a ~1 μm broad band, Fe/Mg phyllosilicates with a ~2.3 μm absorption band, and hydrated silica with a broad 2.2 μm absorption (Figure 2).

Olivine is identified by the broad absorption around 1 μm due to electronic transitions. There are three distinctive occurrences of olivine in the study area, and they are confined to local topographically high units with a close relationship to Fe/Mg phyllosilicates.

Fe/Mg phyllosilicates are detected by the 2.3 μm absorption, caused by Fe-OH or Mg-OH vibrations, along with absorption features at 1.4 μm due to the first overtone of OH vibration and 1.9 μm due to H₂O combination modes. They most likely fall into the smectite group, where the Fe end-member of the smectite group (nontronite) has a band centered at 2.29 μm, while the Mg end-member (saponite) is centered at 2.31–2.32 μm (Figure 2a) [Hunt, 1977; Bishop et al., 2002a; Clark et al., 1990; Frost et al., 2002]. The CRISM data reported here fall in between those two end-members. Materials with similar spectral properties are widespread in the southern highlands [Ehlmann et al., 2009, 2011; Poulet et al., 2007; Carter et al., 2013], including elsewhere in Arabia Terra near the dichotomy boundary [Noe Dobrea et al., 2010]. There are also strong variations in the depth of 1.9 μm absorption band, indicating variability in H₂O content. Differences in the slope of the spectra shortward of 1.9 μm are possibly due to mixture with a ferrous component, e.g., ferrous olivine that is found in the vicinity, or another Fe-bearing alteration mineral [Bishop et al., 2008; McKeown et al., 2009].

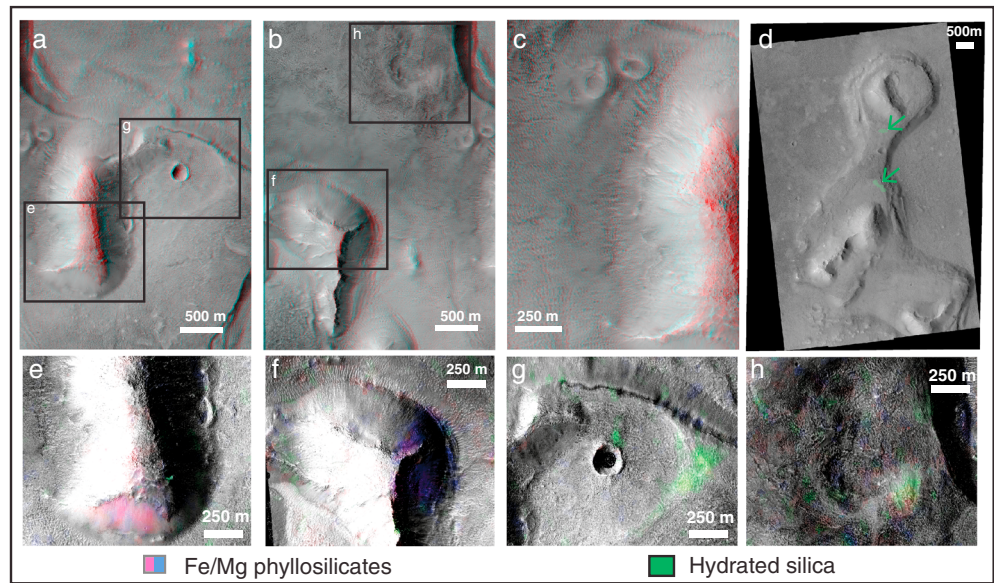


Figure 3. Unit relationship shown on HiRISE imagery. (a, b) Stereo anaglyph images from HiRISE PSP_009985_2205 and PSP_009708_2205 over the same region as CRISM image FRT0000979D. (c) Zoomed-in HiRISE stereo showing the embayment relationship between the surrounding plains unit (left) and the knobs (right). (d) Occurrences of hydrated silica in HiRISE image PSP_002166_2205 with mineral identified from CRISM FRT00017F45. (e, f) The occurrences of Fe/Mg phyllosilicates on the slope of knobs. Hydrated silica detections are found at some locations within the surrounding plains unit, occurring (g) near an impact crater, (h) on local topographical high, and on inflection points of slopes in the plain unit (Figure 3d).

Hydrated silica is detected in three images in the Acidalia region (Figure 1) identified by a characteristic vibrational absorption band at $\sim 2.21 \mu\text{m}$ (Figure 2b), caused by overlapping bands at 2.21 and $2.26 \mu\text{m}$ from Si-OH and H-bound Si-OH, respectively [Anderson and Wickersheim, 1964; Milliken et al., 2008; Skok et al., 2010; Ehlmann et al., 2009]. Absorptions at 1.4 and $1.9 \mu\text{m}$ due to H_2O are also present. The CRISM data all show a characteristic wide $2.2 \mu\text{m}$ absorption extending from 2.16 to $2.41 \mu\text{m}$, distinct from Al-OH vibrational absorptions (e.g., in montmorillonite), which are much narrower (Figure 2b). Studies of laboratory reflectance spectra [Anderson and Wickersheim, 1964; Rice et al., 2013] of silica-rich materials show that the H_2O content and form of $\text{H}_2\text{O}/\text{OH}$ present in silica-rich materials can significantly affect the band center (e.g., 1.41 to $1.38 \mu\text{m}$) and band ratios (e.g., $2.21/2.26 \mu\text{m}$) of major absorption features, for example, allowing hydrated glass to be distinguished from opal. We observe shifts in the absorption near $1.4 \mu\text{m}$ in the CRISM spectra, possibly related to differences in the form of $\text{H}_2\text{O}/\text{OH}$ in the high-silica phase (Figure 2b). However, in Acidalia, CO_2 atmospheric bands obscure the details of the $1.9 \mu\text{m}$ absorptions, and the 1.4 and $2.2 \mu\text{m}$ band centers occur at wavelengths found in multiple types of high-silica phases, so we are not able to make unique interpretation of hydrated silica phase from the spectral analysis.

In one location, among the hydrated minerals mapped with the band depth at $2.2 \mu\text{m}$ (Figure 2b), is a spectrum similar to “doublet material” found in Valles Marineris [Roach et al., 2010] with absorption features at $\sim 1.42 \mu\text{m}$, $\sim 1.92 \mu\text{m}$, and a sharp doublet at $2.205\text{--}2.218 \mu\text{m}$ and $2.265\text{--}2.278 \mu\text{m}$. Mixtures of Fe/Mg smectite and hydrated silica were considered as both are end-members present in our scene, but the Fe/Mg-OH wavelength center is at longer wavelengths. Sulfates like jarosite seem to be a close match, but the doublet is shifted to longer wavelengths in CRISM data versus terrestrial laboratory data. A plausible model would be poorly crystalline Fe-SiO₂ phase due to either acid leaching or neoformation of a smectite as proposed in Roach et al. [2010].

5. Geomorphic Setting

In the survey of Acidalia Planitia, of special interest are the three images with hydrated mineral detections. Within the knobby terrains, three morphologically different units can be discerned on the basis of distinct morphology and mineralogy (Figures 2c, 3a, and 3b). The first unit consists of the knobs where Fe/Mg phyllosilicates and olivine are detected in discontinuous patches on the slope and ridges (Figures 3e–3f; see

Figures 3a and 3b for context) with no detections on the surrounding units. Olivine is also found within a 2.5 km east-west linear feature (~100 m higher than surrounding unit according to Mars Orbiter Laser Altimeter and the HiRISE digital elevation model (DEM)). Detections of both Fe/Mg phyllosilicates and olivine are patchily distributed in the knobs rather than pervasively. There is no preferred direction on the knob for Fe/Mg phyllosilicates or olivines to occur, and no obvious cover is being removed to reveal smectite or olivine-bearing materials, which indicate the patchiness may be a characteristic of the bedrock itself.

The knobs are embayed by a surrounding steep-sided plains unit (Figure 3c), which forms a platform around the knobs and within which the hydrated silica is detected (Figures 3a and 3b). There is no silica detection related to the knobs themselves. Instead, silica is restricted to local topographic highs or inflections in slope in the lower unit that embays the knobs. The detections themselves are discontinuous and patchy (Figures 3d, 3g, and 3h), but the overall distribution extends to three CRISM images ~160 km apart. The occurrence of the “doublet” material coexists with hydrated silica in the unit embaying the knobs.

In total there are nine discrete detections of Fe/Mg phyllosilicates and 11 detections of hydrated silica in the high-resolution data from the 300 km² study area. The total area of Fe/Mg phyllosilicates covers about 1.041 km² and hydrated silica ~0.71 km². The third unit is the overlying smooth plains unit with subkilometer cones, which is the youngest terrain in this region and has no hydrated mineral detections.


6. Discussion

Two hypotheses for the formation of the knobs have been proposed: terrestrial tuyas (emergent subice volcanoes) or eroded remnants of the southern highlands-northern lowlands topographic dichotomy. Tuya formation was recently proposed because some of the bigger mesas form in chains with small conical features and might have been formed in a volcanic setting with glacier on top of the surface [Martinez-Alonso *et al.*, 2011]. Extensive alteration to hydrated minerals and pillow lavas would be expected in such a scenario with melting of the ice sheet during eruption, as is typical for terrestrial tuyas [Bishop *et al.*, 2002b]. The observed patchiness of hydrated minerals and existence of apparently unaltered olivine are not consistent with large-scale volcano-ice interaction. On the other hand, Fe/Mg phyllosilicates are the most common hydrated mineral of Noachian southern highland materials, and patchiness of alteration is a characteristic of the highland phyllosilicates [Mustard *et al.*, 2008], perhaps caused by preferential alteration along fractures during hydrothermalism or diagenesis. Consequently, the mineralogical composition is consistent with Acidalia's knobs being eroded Noachian highlands material, in agreement with Tanaka's [2005] geologic mapping. The olivine-rich linear feature might be an eroded remnant of a dike.

The overlying and embaying units are more enigmatic. These units bearing hydrated silica are disconnected with the phyllosilicate-bearing knobs and likely formed in a different aqueous geochemical environment. The observed patchiness of the silica detections might result from the process that generated the hydrated mineral, i.e., concentration in localized areas, or might be the result of detection bias due to mantling or dissimilar rock textures. Here we favor that the detections are revealing the uneven distribution of hydrated silica within the surrounding plains unit, for in HiRISE images no mantling materials are observed, and the surfaces next to the hydrated silica detections with spectrally neutral signatures have similar textures at the resolution of HiRISE images.

Due to the highly mobile nature of silica [McLennan, 2003], the detected hydrated silica could form in multiple types of environments with varying amounts of water (Table 1). These include forming as hydrated silicate glass in volcanic ash/glass deposit [e.g., Stolper, 1982], vapor weathering from acid gases [e.g., Golden *et al.*, 2005; Schiffman *et al.*, 2006; Seelos *et al.*, 2010], thin-film leaching and coating formation [e.g., Chemtob *et al.*, 2010; Golden *et al.*, 2005], in situ silicate weathering with liquid water [e.g., McLennan, 2003; Squyres *et al.*, 2008], and direct precipitation from a silica-saturated water body [e.g., Rodgers *et al.*, 2004; Preston *et al.*, 2008]. For each of these five scenarios, deposit characteristics would differ, in terms of type of silica, thickness, distribution, and relation to topography (Table 1). The observed patchiness and discontinuous nature of silica detections in Acidalia make it unlikely the materials formed as a volcanic ash deposit, or from igneous melts, in which case the silica would be more widely distributed and definitively associated with a particular unit. The occurrence at local topographic highs is not consistent with the hypothesis of direct precipitation in a standing body of water. Therefore the plausible conditions for hydrated silica to form are intermediate with regard to implications for the prevalence of water: vapor weathering, thin-film leaching, or silicate weathering by surface or subsurface

Table 1. Formation Scenarios of Hydrated Silica

Formation Scenarios	Amount of Water	Type of Silica	Continuity	Distribution	Thickness	Topography
Ash/igneous melt	Low	Hydrated silicate glass	Continuous	Regional, related to volcanism	m–km	Fills topography
Vapor weathering		Opal A, Opal C/CT	Discontinuous	Local, related to vapor fissures	μm–mm	Independent of topography
Thin-film leaching		Hydrated silicate glass Opal A, Opal C/CT	Discontinuous	Regional–local	μm–mm	Independent of topography
Silicate weathering		Opal A, Opal C/CT	Patchy to Continuous	Regional–local	mm–m	Follows topographic surface
Direct precipitation		Opal A, Opal C/CT Chalcedony	Continuous	Patchy, depending on water body size	m–km	Concentrated in topographical low

water. The presence of the “doublet” material in the same unit as the hydrated silica may indicate an acidic environment [Roach *et al.*, 2010].

These hydrated minerals have put further constraints on the origin of the knobs and surrounding unit and erosional and depositional processes within the northern plains. The integrated compositional stratigraphy

of the knobby terrains of Acidalia implies a geological history that starts from ancient Noachian crustal materials (Figure 4):

First, ancient Noachian (or pre-Noachian) crust was altered into patchily distributed phyllosilicates. As the dichotomy boundary was modified by mass wasting, impacts, outflow channels, and aeolian processes, the Noachian crust was fractured, eroded into discrete but spatially aggregated knobs, and the overall dichotomy boundary retreated southward. For similar knobby morphology elsewhere, the “fretting” process can be initiated by fractures, subsurface piping, void collapse, or significant aeolian deflation carving into friable sediments [Irwin *et al.*, 2004]. In Acidalia, however, the knobs are likely more competent than friable sediments and have a higher dielectric constant than most of the rest of the lowland materials [Mouginot *et al.*, 2012].

Resurfacing processes including mass wasting and volcanic activity then created sediment and lavas that fill in the northern plains. High-resolution HiRISE stereo images show that the steep-sided platform unit that surrounds the knobs has diverse texture and undulating topography, consistent with a complex sedimentary or volcanic history. Localized aqueous activity resulted in the formation of hydrated silica and the hydrated doublet material in the platform unit that surrounds the knobs. Thin-film leaching, vapor weathering, or in situ

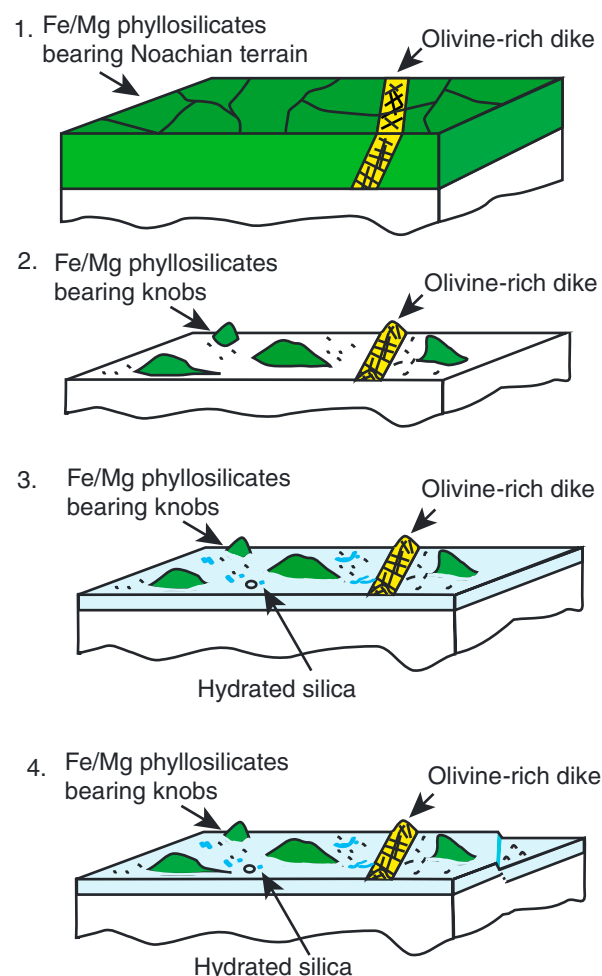


Figure 4. Schematic of the geological history of the knobby terrains in Acidalia.

weathering of silicates in acidic environment may be responsible for the localized aqueous events. The geographic restriction of silica disfavors extensive water bodies (e.g., from interaction with an ocean or an ice sheet), instead favoring environments like springs or steam vents.

Then, sediments undergo collapse and create scarps that define the platform unit that surrounds the knobs. This boundary creates a bench-like morphology and is found to be spatially correlated with local depressions, which are proposed to be formed by volatile-driven collapse and/or basal sapping [Tanaka *et al.*, 2003] rather than wave-cut erosion [Parker *et al.*, 1993]. In this analysis and in previous studies [Farrand *et al.*, 2011; Oehler and Allen, 2010], the topographically lower unit with pitted cones and polygonal troughs lacks hydrated silicate mineral detections, which suggests that the lower unit formed after a decrease in the prevalence or longevity of near-surface liquid water. Collectively, this succession of Noachian, Fe/Mg phyllosilicate-bearing materials, younger hydrated silica-bearing materials, and still younger terrains with no hydrated silicate detections is similar to time succession of minerals found in the southern highlands, in spite of evidence for more volcano-ice interaction and location of the study area within the basin of the proposed northern ocean.

7. Conclusions

Fe/Mg phyllosilicates and hydrated silica have been detected within discrete strata in the knobby terrains in Acidalia and related to units where different morphologic features are present. Fe/Mg phyllosilicates and olivine occur in knobs that are inferred to be eroded remnants from the southern highlands. They are embayed by a platform of surrounding plains with hydrated silica detections, which formed later in a different, possibly more acidic aqueous environment where the availability of water was geographically localized. The hydrated silica detected may have formed via vapor weathering, thin-film leaching, or silicate weathering by liquid water, while the scenarios of volcanic ash/igneous melt deposit and direct precipitation from water bodies are excluded based on the topography and distribution. This study of Acidalia's compositional stratigraphy refines our understanding of the geologic history of Mars' northern plains and together indicates a declining prevalence of aqueous alteration within the northern lowlands through time.

Acknowledgments

Thanks to Jim Skinner for early discussions about northern plains evolution, Ara Oshagan for CTX mosaic and DEM processing, the MRO science operation teams for collecting the data set and the constructive comments of Nancy McKeown and one anonymous reviewer, which improved this manuscript. This work was supported by NASA Mars Data Analysis Program award NNX12AJ43G.

The Editor thanks Nancy McKeown and an anonymous reviewer for their assistance in evaluating this paper.

References

- Anderson, J. H., and K. A. Wickersheim (1964), Near infrared characterization of water and hydroxyl groups on silica surfaces, *Surf. Sci.*, **2**, 252–260, doi:10.1016/0039-6028(64)90064-0.
- Bandfield, J. L., V. E. Hamilton, and P. R. Christensen (2000), A global view of Martian surface compositions from MGS-TES, *Science*, **287**(5458), 1626–1630, doi:10.1126/science.287.5458.1626.
- Bishop, J., J. Madejova, P. Komadel, and H. Froschl (2002a), The influence of structural Fe, Al and Mg on the infrared OH bands in spectra of dioctahedral smectites, *Clay Miner.*, **37**(4), 607–616, doi:10.1180/0009855023740063.
- Bishop, J. L., P. Schiffman, and R. Southard (2002b), Geochemical and mineralogical analyses of palagonitic tuffs and altered rinds of pillow basalts in Iceland and applications to Mars, *Geol. Soc. London Spec. Publ.*, **202**(1), 371–392, doi:10.1144/gsl.sp.2002.202.01.19.
- Bishop, J. L., et al. (2008), Phyllosilicate diversity and past aqueous activity revealed at Mawrth Vallis, Mars, *Science*, **321**(5890), 830–833.
- Carter, J., F. Poulet, J. P. Bibring, and S. Murchie (2010), Detection of hydrated silicates in crustal outcrops in the northern plains of Mars, *Science*, **328**(5986), 1682–1686, doi:10.1126/science.1189013.
- Carter, J., F. Poulet, J. P. Bibring, N. Mangold, and S. Murchie (2013), Hydrous minerals on Mars as seen by the CRISM and OMEGA imaging spectrometers: Updated global view, *J. Geophys. Res. Planets*, **118**, 831–858, doi:10.1029/2012JE004145.
- Carr, M. H., and J. W. Head (2003), Oceans on Mars: An assessment of the observational evidence and possible fate, *J. Geophys. Res.*, **108**(E5), 5042, doi:10.1029/2002JE001963.
- Chemtob, S. M., B. L. Jolliff, G. R. Rossman, J. M. Eiler, and R. E. Arvidson (2010), Silica coatings in the Ka'u Desert, Hawaii, a Mars analog terrain: A micromorphological, spectral, chemical, and isotopic study, *J. Geophys. Res.*, **115**, E04001, doi:10.1029/2009JE003339.
- Christensen, P. R., et al. (2001), Mars Global Surveyor Thermal Emission Spectrometer experiment: Investigation description and surface science results, *J. Geophys. Res.*, **106**(E10), 23,823–23,871, doi:10.1029/2000JE001370.
- Clark, R. N., T. V. V. King, M. Klejwa, and G. A. Swayze (1990), High spectral resolution reflectance spectroscopy of minerals, *J. Geophys. Res.*, **95**(B8), 12,653–12,680.
- Ehlmann, B. L., et al. (2009), Identification of hydrated silicate minerals on Mars using MRO-CRISM: Geologic context near Nili Fossae and implications for aqueous alteration, *J. Geophys. Res.*, **114**, E00d08, doi:10.1029/2009JE003339.
- Ehlmann, B. L., J. F. Mustard, S. L. Murchie, J. P. Bibring, A. Meunier, A. A. Fraeman, and Y. Langevin (2011), Subsurface water and clay mineral formation during the early history of Mars, *Nature*, **479**(7371), 53–60, doi:10.1038/Nature10582.
- Farrand, W. H., L. R. Gaddis, and L. Keszthelyi (2005), Pitted cones and domes on Mars: Observations in Acidalia Planitia and Cydonia Mensae using MOC, THEMIS, and TES data, *J. Geophys. Res.*, **110**, 5005, doi:10.1029/2004JE002297.
- Farrand, W. H., M. D. Lane, B. R. Edwards, and R. A. Yingst (2011), Spectral evidence of volcanic cryptodomes on the northern plains of Mars, *Icarus*, **211**(1), 139–156, doi:10.1016/j.icarus.2010.09.006.
- Frey, H., B. L. Lowry, and S. A. Chase (1979), Pseudo-craters on Mars, *J. Geophys. Res.*, **84**, 8075–8086, doi:10.1029/Jb084ib14p08075.
- Frey, H., and M. Jarosewich (1981), Martian pseudocraters: Searching the northern plains, *Lunar and Planetary Institute Science XII*, pp. 297–299. Abstract.
- Frey, H., and M. Jarosewich (1982), Sub-kilometer Martian volcanos—Properties and possible terrestrial analogs, *J. Geophys. Res.*, **87**(Nb12), 9867–9879, doi:10.1029/Jb087ib12p09867.

- Frey, H. V., J. H. Roark, K. M. Shockey, E. L. Frey, and S. E. H. Sakimoto (2002), Ancient lowlands on Mars, *Geophys. Res. Lett.*, 29(10), 1384, doi:10.1029/2001GL013832.
- Frost, R. L., J. T. Klopogge, and Z. Ding (2002), Near-infrared spectroscopic study of nontronites and ferruginous smectite, *Spectrochim. Acta A*, 58(8), 1657–1668, doi:10.1016/S1386-1425(01)00637-0.
- Golden, D. C., D. W. Ming, R. V. Morris, and S. A. Mertzman (2005), Laboratory-simulated acid-sulfate weathering of basaltic materials: Implications for formation of sulfates at Meridiani Planum and Gusev Crater, Mars, *J. Geophys. Res.*, 110, E12s07, doi:10.1029/2005JE002451.
- Head, J. W., H. Hiesinger, M. A. Ivanov, M. A. Kreslavsky, S. Pratt, and T. B. J. (1999), Possible ancient oceans on Mars: Evidence from Mars Orbiter Laser Altimeter data, *Science*, 286(5447), 2134–2137.
- Head, J. W., M. A. Kreslavsky, and S. Pratt (2002), Northern lowlands of Mars: Evidence for widespread volcanic flooding and tectonic deformation in the Hesperian Period, *J. Geophys. Res.*, 107(E1), 5003, doi:10.1029/2000JE001445.
- Horgan, B., and J. F. Bell III (2012), Widespread weathered glass on the surface of Mars, *Geology*, 40(5), 391–394, doi:10.1130/g32755.1.
- Hunt, G. R. (1977), Spectral signatures of particulate minerals in visible and near infrared, *Geophysics*, 42(3), 501–513, doi:10.1190/1.1440721.
- Irwin, R. P., T. R. Watters, A. D. Howard, and J. R. Zimbelman (2004), Sedimentary resurfacing and fretted terrain development along the crustal dichotomy boundary, Aeolis Mensae, Mars, *J. Geophys. Res.*, 109, E09011, doi:10.1029/2004JE002248.
- Kraft, M. D., J. R. Michalski, and T. G. Sharp (2003), Effects of pure silica coatings on thermal emission spectra of basaltic rocks: Considerations for Martian surface mineralogy, *Geophys. Res. Lett.*, 30(24), 2288, doi:10.1029/2003GL018848.
- Kreslavsky, M. A., and J. W. Head (2002), Fate of outflow channel effluents in the northern lowlands of Mars: The Vastitas Borealis Formation as a sublimation residue from frozen ponded bodies of water, *J. Geophys. Res.*, 107(E12), 5121, doi:10.1029/2001JE001831.
- Lucchitta, B. K. (1981), Mars and Earth—Comparison of cold-climate features, *Icarus*, 45(2), 264–303, doi:10.1016/0019-1035(81)90035-X.
- Malin, M. C., et al. (2007), Context Camera Investigation on board the Mars Reconnaissance Orbiter, *J. Geophys. Res.*, 112, E05s04, doi:10.1029/2006JE002808.
- McEwen, A. S., et al. (2007), Mars Reconnaissance Orbiter's High Resolution Imaging Science Experiment (HiRISE), *J. Geophys. Res.*, 112, E05s02, doi:10.1029/2005JE002605.
- McKeown, N. K., J. L. Bishop, E. Z. N. Dobrea, B. L. Ehlmann, M. Parente, J. F. Mustard, S. L. Murchie, G. A. Swayze, J. P. Bibring, and E. A. Silver (2009), Characterization of phyllosilicates observed in the central Mawrth Vallis region, Mars, their potential formational processes, and implications for past climate, *J. Geophys. Res.*, 114, doi:10.1029/2008JE003301.
- McGill, G. E. (2005), Geologic map of Cydonia Mensae-southern Acidalia Planitia, Mars: Quadrangles 40007, 40012, 40017, 45007, 45012, and 45017, U.S. Geol. Survey, Geol. Invest. Map I-2811.
- McLennan, S. M. (2003), Sedimentary silica on Mars, *Geology*, 31(4), 315–318, doi:10.1130/0091-7613(2003)031<0315:SSom>2.0.CO;2.
- Martinez-Alonso, S., M. T. Mellon, M. E. Banks, L. P. Keszthelyi, A. S. McEwen, and H. Team (2011), Evidence of volcanic and glacial activity in Chryse and Acidalia Planitiae, Mars, *Icarus*, 212(2), 597–621, doi:10.1016/J.Icarus.2011.01.004.
- Michalski, J. R., M. D. Kraft, T. G. Sharp, L. B. Williams, and P. R. Christensen (2005), Mineralogical constraints on the high-silica Martian surface component observed by TES, *Icarus*, 174(1), 161–177, doi:10.1016/J.Icarus.2004.10.022.
- Milliken, R. E., et al. (2008), Opaline silica in young deposits on Mars, *Geology*, 36(11), 847–850, doi:10.1130/G24967a.1.
- Moratto, Z. M., Broxton, M. J., Beyer, R. A., Lundy, M. and K. Husmann (2010), Ames Stereo Pipeline, NASA's Open Source Automated Stereogrammetry software, 41st LPSC, 2364.
- Mouginot, J., A. Pommerol, P. Beck, W. Kofman, and S. M. Clifford (2012), Dielectric map of the Martian northern hemisphere and the nature of plain filling materials, *Geophys. Res. Lett.*, 39, L02202, doi:10.1029/2011GL050286.
- Murchie, S. L., et al. (2009), Compact Reconnaissance Imaging Spectrometer for Mars investigation and data set from the Mars Reconnaissance Orbiter's primary science phase, *J. Geophys. Res.*, 114, E00d07, doi:10.1029/2009JE003344.
- Mustard, J. F., F. Poulet, A. Gendrin, J. P. Bibring, Y. Langevin, B. Gondet, N. Mangold, G. Bellucci, and F. Altieri (2005), Olivine and pyroxene, diversity in the crust of Mars, *Science*, 307(5715), 1594–1597, doi:10.1126/science.1109098.
- Mustard, J. F., et al. (2008), Hydrated silicate minerals on Mars observed by the Mars reconnaissance orbiter CRISM instrument, *Nature*, 454(7202), 305–309, doi:10.1038/Nature07097.
- Nimmo, F., and K. Tanaka (2005), Early crustal evolution of Mars, *Annu. Rev. Earth Planet. Sci.*, 33, 133–161, doi:10.1146/Annurev.Earth.33.092203.122637.
- Noe Dobrea, E. Z., et al. (2010), Mineralogy and stratigraphy of phyllosilicate-bearing and dark mantling units in the greater Mawrth Vallis/west Arabia Terra area: Constraints on geological origin, *J. Geophys. Res.*, 115, E00D19, doi:10.1029/2009JE003351.
- Oehler, D. Z., and C. C. Allen (2010), Evidence for pervasive mud volcanism in Acidalia Planitia, Mars, *Icarus*, 208(2), 636–657, doi:10.1016/J.Icarus.2010.03.031.
- Parker, T. J., D. S. Gorsline, R. S. Saunders, D. C. Pieri, and D. M. Schneeberger (1993), Coastal geomorphology of the Martian northern plains, *J. Geophys. Res.*, 98(E6), 11,061–11,078, doi:10.1029/93JE00618.
- Pelkey, S. M., et al. (2007), CRISM multispectral summary products: Parameterizing mineral diversity on Mars from reflectance, *J. Geophys. Res.*, 112, E08s14, doi:10.1029/2006JE002831.
- Poulet, F., C. Gomez, J.-P. Bibring, Y. Langevin, B. Gondet, P. Pinet, G. Bellucci, and J. Mustard (2007), Martian surface mineralogy from Observatoire pour la Minéralogie, l'Eau, les Glaces et l'Activité on board the Mars Express spacecraft (OMEGA/MEX): Global mineral maps, *J. Geophys. Res.*, 112, E08S02, doi:10.1029/2006JE002840.
- Preston, L. J., G. K. Benedix, M. J. Genge, and M. A. Sephton (2008), A multidisciplinary study of silica sinter deposits with applications to silica identification and detection of fossil life on Mars, *Icarus*, 198(2), 331–350, doi:10.1016/J.Icarus.2008.08.006.
- Rice, M. S., E. A. Cloutis, J. F. Bell, D. L. Bish, B. H. Horgan, S. A. Mertzman, M. A. Craig, R. W. Renaut, B. Gautason, and B. Mountain (2013), Reflectance spectra diversity of silica-rich materials: Sensitivity to environment and implications for detections on Mars, *Icarus*, 223(1), 499–533, doi:10.1016/J.Icarus.2012.09.021.
- Roach, L. H., J. F. Mustard, G. Swayze, R. E. Milliken, J. L. Bishop, S. L. Murchie, and K. Lichtenberg (2010), Hydrated mineral stratigraphy of Ius Chasma, Valles Marineris, *Icarus*, 206(1), 253–268, doi:10.1016/J.Icarus.2009.09.003.
- Rodgers, K. A., et al. (2004), Silica phases in sinters and residues from geothermal fields of New Zealand, *Earth Sci. Rev.*, 66(1–2), 1–61, doi:10.1016/j.earscirev.2003.10.001.
- Salvatore, M. R., J. F. Mustard, M. B. Wyatt, and S. L. Murchie (2010), Definitive evidence of Hesperian basalt in Acidalia and Chryse Planitiae, *J. Geophys. Res.*, 115, E07005, doi:10.1029/2009JE003519.
- Seelos, K. D., R. E. Arvidson, B. L. Jolliff, S. M. Chemtob, R. V. Morris, D. W. Ming, and G. A. Swayze (2010), Silica in a Mars analog environment: Ka'u Desert, Kilauea Volcano, Hawaii, *J. Geophys. Res.*, 115, E00d15, doi:10.1029/2009JE003347.
- Schiffman, P., R. Zierenberg, N. Marks, J. L. Bishop, and M. D. Dyar (2006), Acid-fog deposition at Kilauea Volcano: A possible mechanism for the formation of siliceous-sulfate rock coatings on Mars, *Geology*, 34(11), 921–924, doi:10.1130/G22620a.1.

- Skok, J. R., J. F. Mustard, S. L. Murchie, M. B. Wyatt, and B. L. Ehlmann (2010), Spectrally distinct ejecta in Syrtis Major, Mars: Evidence for environmental change at the Hesperian-Amazonian boundary, *J. Geophys. Res.*, **115**, E00D14, doi:10.1029/2009JE003338.
- Squyres, S. W., et al. (2008), Detection of silica-rich deposits on Mars, *Science*, **320**(5879), 1063–1067, doi:10.1126/Science.1155429.
- Stolper, E. (1982), Water in silicate glasses: An infrared spectroscopic study, *Contrib. Mineral. Petrol.*, **81**, 1–17, doi:10.1007/BF00371154.
- Tanaka, K. L. (1997), Sedimentary history and mass flow structures of Chryse and Acidalia Planitiae, Mars, *J. Geophys. Res.*, **102**(E2), 4131–4149, doi:10.1029/96JE02862.
- Tanaka, K. L., W. B. Banerdt, J. S. Kargel, and N. Hoffman (2001), Huge, CO₂-charged debris-flow deposit and tectonic sagging in the northern plains of Mars, *Geology*, **29**(5), 427–430.
- Tanaka, K. L., J. A. Skinner, T. M. Hare, T. Joyal, and A. Wenker (2003), Resurfacing history of the northern plains of Mars based on geologic mapping of Mars Global Surveyor data, *J. Geophys. Res.*, **108**(E4), 8043, doi:10.1029/2002JE001908.
- Tanaka, K. L., J. A. Skinner, and T. M. Hare (2005), Geologic Map of the northern plains of Mars, U.S. Department of Interior, U.S. Geological Survey.
- Wyatt, M. B., and H. Y. McSween (2002), Spectral evidence for weathered basalt as an alternative to andesite in the northern lowlands of Mars, *Nature*, **417**, 263–266.